Research article

Journal of RAMAN SPECTROSCOPY

Received: 4 September 2013 Revised: 6 December 2013 Accepted: 7 December 2013 Published online in Wiley Online Library: 20 January 2014

(wileyonlinelibrary.com) DOI 10.1002/jrs.4442

In-situ Raman spectroscopy of current-carrying graphene microbridge

Minkyung Choi,[a†] Jangyup Son,[b†] Heechae Choi,[c] Hyun-Joon Shin,[d] Sangho Lee,[b] Sanghoon Kim,[b] Soogil Lee,[b] Seungchul Kim,[c] Kwang-Ryeol Lee,[c] Sang Jin Kim,[e] Byung Hee Hong,[e] Jongill Hong[b]* and In-Sang Yang[a]*

***In-situ* Raman spectroscopy was performed on chemical vapor deposited graphene microbridge (3 μm × 80 μm) under electrical current density up to 2.58×10^8 A/cm^2 in ambient conditions. We found that both the G and the G′ peak of the Raman spectra do not restore back to the initial values at zero current, but to slightly higher values after switching off the current through the microbridge. The up-shift of the G peak and the G′ peak, after switching off the electrical current, is believed to be due to p-doping by oxygen adsorption, which is confirmed by scanning photoemission microscopy. Both C–O and C=O bond components in the C1*s* spectra from the microbridge were found to be significantly increased after high electrical current density was flown. The C=O bond is likely the main source of the p-doping according to our density functional theory calculation of the electronic structure. Copyright © 2014 John Wiley & Sons, Ltd.**

Additional supporting information may be found in the online version of this article at the publisher's web site.

Keywords: *in-situ* Raman spectroscopy; graphene; Joule heating; doping

Introduction

Graphene has many two-dimensional extraordinary features, which makes it promising for future electronic devices.[1–3] Since it was experimentally realized in 2004, graphene has been the object of intense theoretical and experimental research due to its exceptional electrical, physical, and chemical properties.[4–10] Because graphene is a zero-gap material with the linear dispersion at the Fermi energy (E_F) and with its peculiar electronic characteristics,[4,5] such as electric-field effects and high carrier mobility,[6–10] it can be an ideal candidate for not only nano-electronic devices but also chemical and biological sensors.[11–15]

For applications, graphene should be produced in a large scale by a controllable manner, such as a chemical-vapor-deposition (CVD) method.[16–18] However, unlike the graphene exfoliated from graphite, the CVD-grown graphene is not free from defects which can be chemically reactive.[19] When graphene device is under operation, therefore, graphene can experience a substantial modification in chemical and electrical properties, particularly due to heating by the electro-thermal effect.[20] Naturally, we need to know what would happen to an electronic circuit made of graphene when an electrical current flows under natural conditions such as in air. Research on graphene-based nanoelectronic applications has been extensive, but little progress has been made under practical operating conditions such as under electrical current as high as that at which graphene starts to breakdown. In addition, most experiments contributing to the advance in science and technologies of graphene have been carried out in vacuum, an ideal condition.[21,22] The gases and other species in air have kept researchers from studying graphene's electrical behavior at its breakdown limit.[23] Further understanding of the behavior of graphene in those harsh and realistic environments is essential to realize a new era of graphene electronics in near future.

Raman spectroscopy is a powerful non-destructive technique for identifying the number of layers, stress, electron−phonon interaction, and disorder of graphene.[24–28] The most notable features of Raman spectrum of graphene are the G peak at 1580 cm^{-1} and the relatively wide G′ peak around 2700 cm^{-1}. The G peak and the G′ peak are strongly dependent on the local temperature and the doping condition of graphene.[22,26,29]

In this work, we performed *in-situ* Raman measurements on a CVD graphene microbridge on SiO_2/Si substrates, in air under

* *Correspondence to: In-Sang Yang, Department of Physics, Ewha Womans University, Seoul 120-750, Korea.*
E-mail: yang@ewha.ac.kr
* *Correspondence to: Jongill Hong, Department of Materials Science and Engineering, Yonsei University, Seoul 120-749, Korea.*
E-mail: hong.jongill@yonsei.ac.kr

† *These authors contributed equally.*

a *Department of Physics, Ewha Womans University, Seoul, 120-750, Korea*

b *Department of Materials Science and Engineering, Yonsei University, Seoul, 120-749, Korea*

c *Center for Computational Science, Korea Institute of Science and Technology, Seoul, 136-791, Korea*

d *Pohang Accelerator Laboratory, Pohang, 790-784, Korea*

e *Department of Chemistry, College of Natural Sciences, Seoul National University, Seoul, 151-747, Korea*

Journal of RAMAN SPECTROSCOPY

electrical current density up to 2.58×10^8 A/cm^2. We report our experimental and theoretical findings about what is happening to the microbridge of CVD-grown graphene, a primitive graphene electronic device, when the high-density electrical currents flow in ambient conditions.

Experimental

Graphene was synthesized through the chemical vapor deposition (CVD) method on a high purity copper catalyst (Alpha aecer, 99.999%) under H_2 condition (70 mtorr, 3 sccm) with methane used as a hydrocarbon source (650 mtorr, 30 sccm). We used Cu substrates alloyed with ~ 1% Ag to suppress the formation of multilayer graphene.[16] As-grown graphene on a Cu substrate was spin-coated with polymethylmethacrylate (PMMA) and backside graphene was etched using oxygen plasma. The Cu substrate was finally etched in 1.5 wt.% ammonium persulfate (APS) solution. After several rinsing processes in distilled water, graphene was transferred on an electrode-patterned 300 nm thick SiO_2/heavily p-doped Si wafer. Subsequently, the coated-PMMA layer was removed by acetone and the sample was annealed at 350 °C with argon and hydrogen condition to remove the remained polymer residues.[18]

The electron diffraction pattern in Fig. 1a shows that our graphene was indeed a single layer with a hexagonal symmetry and a lattice parameter of 2.46 Å. Raman spectroscopy has been used to identify the number of a graphene layer, doping, and damages on graphene after the fabrication process.[24–26] The weak

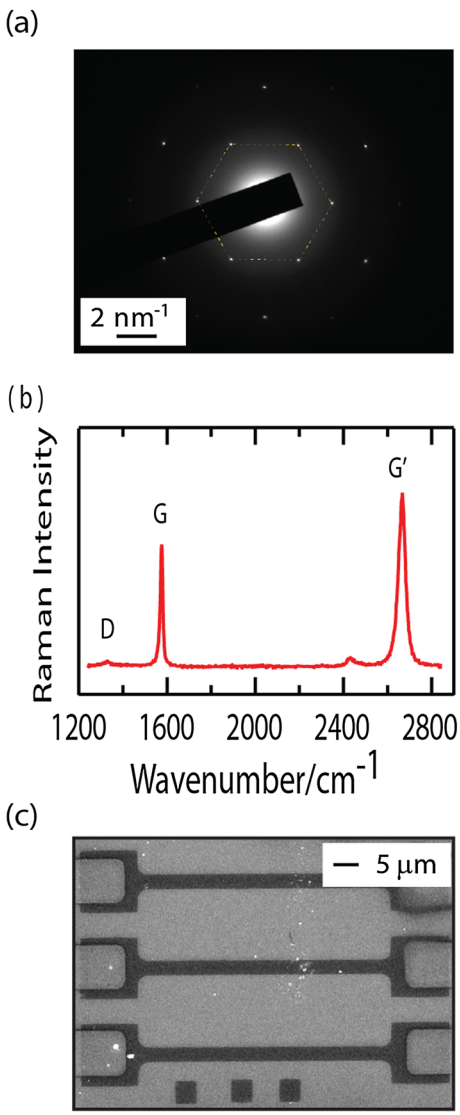

Figure 1. Characterization of our graphene and the geometry of the graphene microbridge. (a) The electron diffraction pattern and (b) the Raman spectrum of the CVD graphene, and (c) the scanning electron microscopic (SEM) image of the graphene microbridge with a dimension of 3×80 μm^2. The three dark small squares at the bottom (called windows) in the SEM image serve as reference in our Raman and XPS measurements.

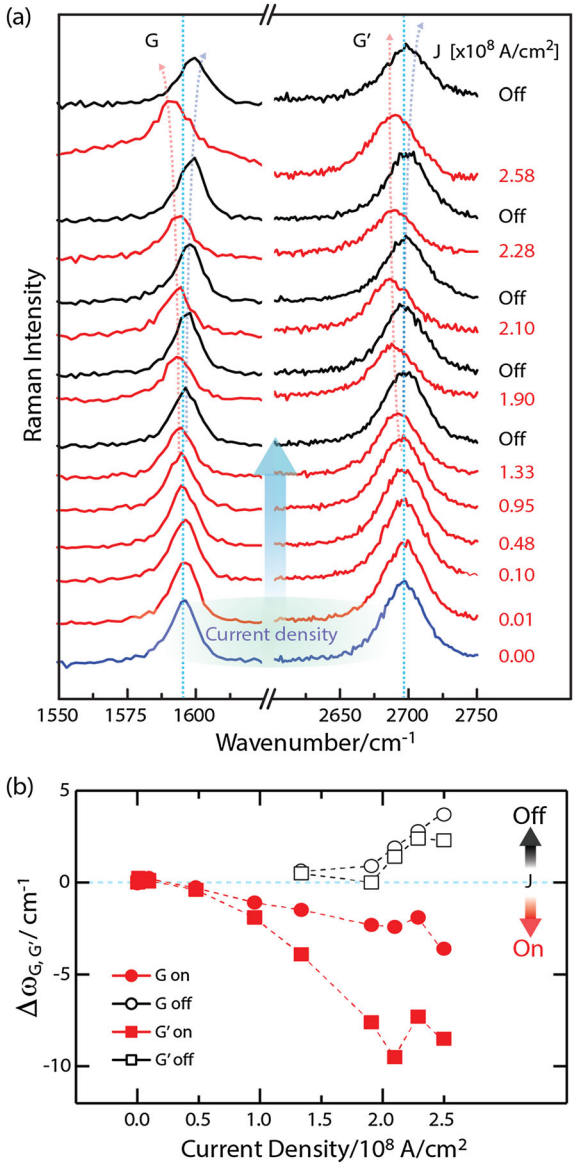

Figure 2. Evolution of Raman spectra of the graphene microbridge as a function of applied current densities. (a) Raman spectra under various current densities from zero to 2.58×10^8 A/cm^2. The blue curve is the Raman spectrum at the initial state; the red curves are the spectra under the electrical current density as indicated; the black curves are the spectra after the current is turned off. The blue dotted lines show the positions of the G and the G′ peak at the initial state. (b) The shift in the G and the G′ peak ($\Delta\omega_{G,G'}$) at various current densities. The upper and lower parts of the graph show the shifts in the wavenumber of the G and the G′ peak when the electrical current is off and on, respectively. This figure is available in colour online at wileyonlinelibrary.com/journal/jrs

D-peak (~1340 cm^{-1}) intensity of graphene clearly indicates that our graphene was nearly free of damages after fabrication (Fig. 1b). Graphene microbridges (3 μm × 80 μm), as shown in Fig. 1c, were fabricated by transferring graphene on top of a SiO_2 substrate with Ti/Pt electrodes, patterning an etch mask with electron-beam lithography, and etching with O_2 plasma (see the supplementary information.) The three small squares at the bottom in Fig. 1c are called windows, and they serve as reference in our measurements.

The Raman spectra were recorded with a Horiba Jobin-Yvon LabRam HR spectrometer and detected with a liquid-nitrogen-cooled CCD detector. The 514.5 nm line of an Ar ion laser was used as the excitation source, and a laser power on the sample was kept around 100 μW, to avoid heating of the sample during the measurements. The Raman scattered light signal was collected in a backscattering geometry using a long-working distance microscope objective lens (×50, 0.5 N.A.). The Raman spectra were taken from the center of the graphene microbridge where the Joule heating effect is expected to be the strongest,[30] by focusing the Raman excitation beam onto an ~1 μm diameter spot. The Raman spectra from the window region served as reference. Each Raman acquisition time was 2 min, and there were off-current intervals of about 2 min between each step.

Results and discussion

Fig. 2a shows the Raman spectra of the graphene microbridge, taken as the current density was varied as indicated. *In-situ* Raman measurements were performed on the graphene microbridge in air before any current was flowing (blue line) and while the current was flowing (red line). We observed down-shift of the G and G′ peaks during the application of

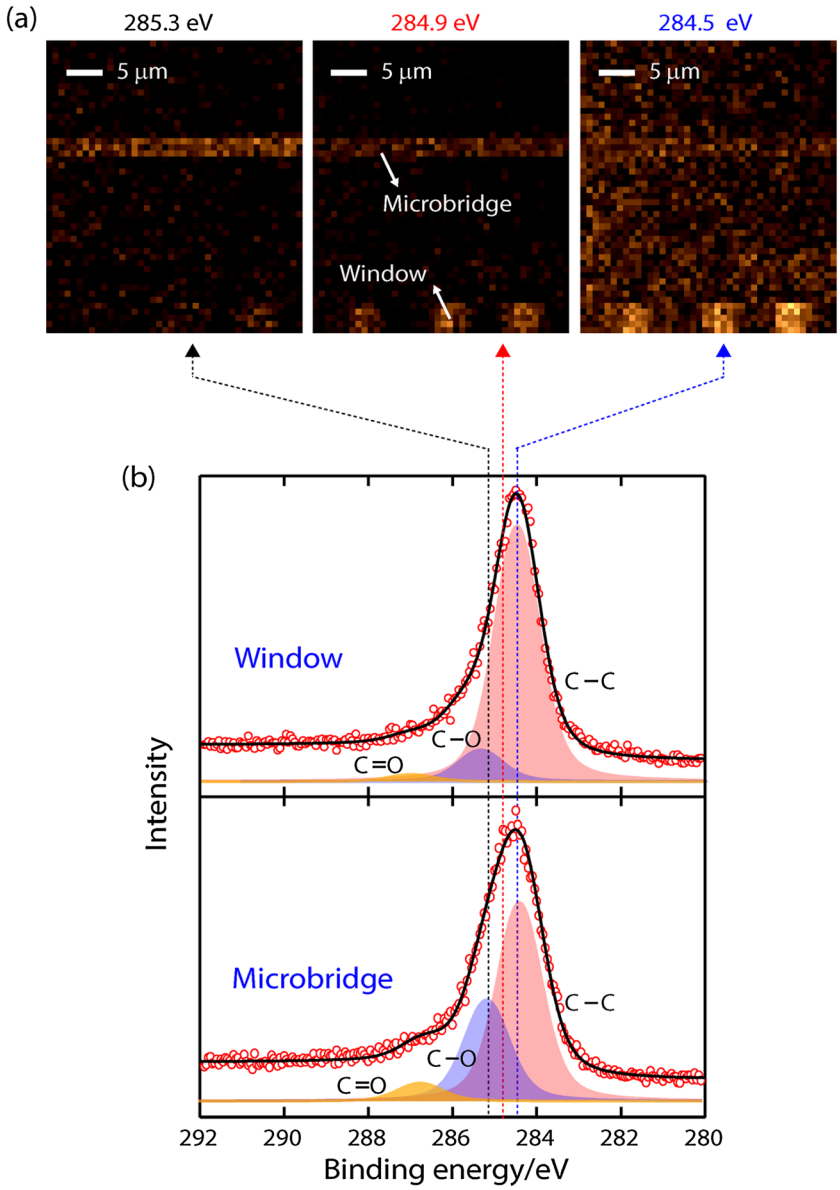

Figure 3. SPEM images and XPS spectra of the window and the microbridge regions. (a) SPEM images of the graphene microbridge simultaneously measured at different values of binding energy of C1*s*: 285.3, 284.9, and 284.5 eV. (b) Photoemission spectra of the C1*s* core-level from the window region (up) and the microbridge region (down). Open circles, solid black lines, and red, blue, and yellow areas indicate raw data, fitted curves, and the integrated intensity areas of C–C, C–O, and C=O bonding, respectively. This figure is available in colour online at wileyonlinelibrary.com/journal/jrs

Journal of RAMAN SPECTROSCOPY

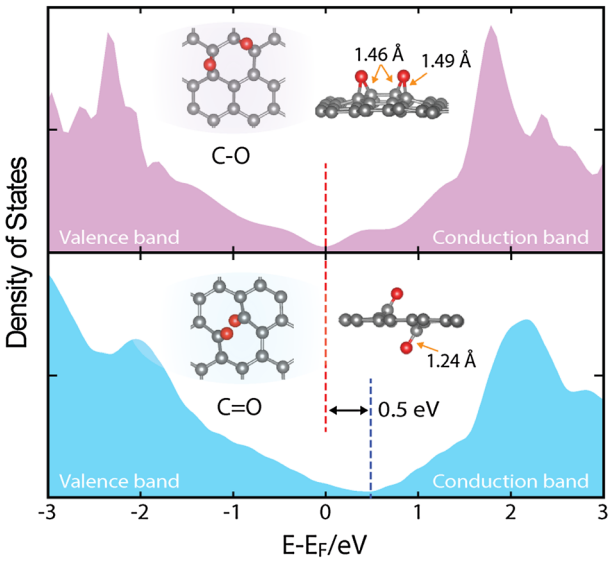

Figure 4. The density of states (DOS) for possible configurations of C–O and C=O bonds. The O-adsorbed graphene supercells with an 8×8 size were calculated. The dashed red and blue vertical lines indicate the Fermi level of graphene and the shifted Dirac point of graphene with C=O, respectively. The p-doping of graphene by O adsorption is mainly caused by the C=O bond by a shift of ~0.5 eV in the Dirac point above the Fermi level. This figure is available in colour online at wileyonlinelibrary.com/journal/jrs

currents, which happened without any noticeable increase in the D peak intensity. The down-shift of the G and the G′ peak is most likely due to Joule heating.[21,30] Ni *et al.* reported that the G and the G′ peak down-shift at high temperature, and their temperature coefficients are −0.019 and −0.051 cm^{-1}/°C, respectively.[31] Calizo *et al.* also reported the coefficient −0.016 cm^{-1}/°C in the temperature range between −190 and 100 °C.[29] In our results, the down-shift of G and G′ peaks was about 4 and 8 cm^{-1}, respectively, at the current density of 2.58×10^8 A/cm^2. We estimated the temperature to be over 200 °C at the current density of 2.58×10^8 A/cm^2 by the G peak's temperature coefficient given in Ref..[31]Notice that the zero-current Raman spectra (black lines) of the graphene microbridge heated at high current density (from 1.33 to 2.58×10^8 A/cm^2) are significantly different from the initial spectra (blue line) after turning off the currents. The wavenumber shift of the G and the G′ peak ($\Delta\omega_{G,\,G'}$) at various current densities is plotted in Fig. 2b when the electrical current was switched on and off. Note the up-shift of the G and the G′ peak right after turning off the electrical currents as denoted. The up-shift of the Raman G peak is widely interpreted as a measure of carrier doping. The G peak can up-shift due either to the application of compressive strain,[32,33] or to electrical doping.[26,34] Das. *et al.* reported that the G peak stiffens by both electron and hole doping and the G′ peak responds differently to holes and electrons.[26] Ryu *et al.* reported that the observed up-shift in both initially exfoliated and annealed graphene is principally due to O_2 induced hole-doping rather than in-plane compressive strain, using environment-controlled *in-situ* Raman spectroscopy measurements.[34]

Our Raman results, along with the photoemission spectroscopy results as following, clearly indicate that the up-shift of G and G′ peaks is due to the adsorption of oxygen onto the Joule-heated graphene surfaces. Doping changes the Fermi level and then moves the Kohn anomaly away from $q=0$. Therefore, the G peak position of graphene is renormalized by the doping level. Figure 2b shows that the doping level was dependent on the Joule heating power at the instance that the microbridge was subjected to just before turning off the electrical current flow.

Scanning photoemission microscopy (SPEM) and X-ray photoelectron microscopy (XPS), as shown in Fig. 3, prove the adsorption of oxygen onto the Joule-heated graphene surface in an ambient condition. The XPS survey scan revealed that oxygen is the predominant species in the graphene microbridge experiencing electrical heating. Spectra of other species were too weak to be detected in the scan. A scanning focused beam with a diameter of ~1 μm at a photon energy of 630 eV was used to compare the chemical states of the surface of graphene in the microbridge and in the windows, respectively (indicated in the middle image of Fig. 3a). Adsorbed oxygen in the graphene microbridge was observed after the electrical breakdown current limit was surpassed. Figure 3a shows the SPEM images of our graphene device at three different binding energies of C1*s*, 284.5, 284.9, and 285.3 eV. The color contrast displays relative intensities of the denoted peaks in each region. The graphene in the microbridge showed uniform changes throughout the surface, while graphenes in the window remained intact as pristine graphene since they were electrically isolated from the microbridge. At the binding energy of 284.5 eV corresponding to the C–C binding energy,[35] the window regions were brighter than the other regions. As the binding energy increased up to 285.3 eV, which corresponds to the binding energy of the C–O bonds,[36] the microbridge became gradually brighter than the windows. The fine structure of C1*s* analyzed by XPS clarifies that C–O and C=O bonds were substantial in the microbridge whereas they were insignificant in the window, as shown in Fig. 3b. After the flow of high density electrical currents, the C=O peak area increased from 2.4% in the window to 5.7% in the microbridge. It is clear that the whole surface of the graphene microbridge was oxidized by the electrothermal effect.

The density of states (DOS) of graphene for the possible C–O and C=O bond configurations as shown in Fig. 4 were obtained using density functional theory (DFT) calculations as implemented in the Vienna Ab-initio Simulation Package (VASP) code.[37] Based on energetics, we chose two configurations for the absorption of oxygen atoms: (1) a C–O bond in which adsorbed O atoms take the bridge site between two C atoms of graphene (the upper panel) and (2) a C=O bond which one O atom on one side and another O atom on the other side of graphene form (the lower panel). The DOS of the graphene with the C–O bond turned out to have a symmetric curve, which is similar to that of the pristine graphene. Therefore, it should be irrelevant with a significant shift in the Dirac point or with p-doping. On the other hand, our calculation disclosed that the C=O configuration on graphene shifts the Dirac point above the Fermi level by 0.5 eV, as shown in Fig. 4, which demonstrates the dominant role of the C=O bond in the p-doping of graphene.

Conclusion

In summary, we performed an *in-situ* Raman measurement on chemical vapor deposited graphene microbridge under high electrical current density up to 2.58×10^8 A/cm^2. We found that the G and the G′ peak are higher than the initial values at zero current after switching off the current through the microbridge. The up-shift of the G and the G′ peak right after turning off electrical currents indicates the p-doping of graphene, possibly by the adsorption of oxygen. The adsorption of oxygen is

confirmed by scanning photoemission microscopy. The density functional theory calculation of the electronic structure reveals that the C=O bond is responsible for the p-doping of the graphene microbridge.

Acknowledgements

We thank Prof. S. J. Oh of Seoul National University for his helpful comments on XPS results. Research at Ewha Womans University was supported in part by the National Research Foundation of Korea (NRF) grant funded by the Korea government (MSIP) (No.2008-0061893). Research at Yonsei University was supported in part by Samsung Electronics Co.; Basic Science Research Program through the National Research Foundation of Korea funded by the Ministry of Education (NRF-2013R1A1A2013745), the Pioneer Research Center Program (2013-008914), the Ministry of Science, ICT and Future Planning, and the Pohang Accelerator Laboratory (SM-12), XFEL project, Korea; and the Future Semiconductor Device Technology Development Program (10044723) funded by the Ministry of Trade, Industry and Energy and the Korea Semiconductor Research Consortium. Works at KIST was supported by the Converging Research Center Program through the Ministry of Science, IT, and Future Planning (Grant Number 2012K001314).

References

[1] K. S. Novoselov, A. K. Geim, S. V. Morozov, D. Jiang, Y. Zhang, S. V. Dubonos, I. V. Grigorieva, A. A. Firsov, *Science* **2004**, *306*, 666.
[2] K. S. Novoselov, A. K. Geim, S. V. Morozov, D. Jiang, M. I. Katsnelson, I. V. Grigorieva, S. V. Dubonos, A. A. Firsov, *Nature* **2005**, *438*, 197.
[3] Y. Zhang, Y. Tan, H. L. Stormer, P. Kim, *Nature* **2005**, *43*, 201.
[4] A. H. Castro Neto, F. Guinea, N. M. R. Peres, K. S. Novoselov, A. K. Geim, *Rev. Mod. Phys.* **2009**, *81*, 109.
[5] S. Das Sarma, S. Adam, E. H. Hwang, E. Rossi, *Rev. Mod. Phys.* **2011**, *83*, 407.
[6] J. H. Chen, C. Jang, S. D. Xiao, M. Ishigami, M. S. Fuhrer, *Nat. Nanotechnol.* **2008**, *3*, 206.
[7] K. I. Bolotin, K. J. Sikes, Z. Jiang, M. Klima, G. Fudenberg, J. Hone, P. Kim, H. L. Stormer, *Sol. State Commun.* **2008**, *146*, 351.
[8] S. V. Morozov, K. S. Novoselov, M. I. Katsnelson, F. Schedin, D. C. Elias, J. A. Jaszczak, A. K. Geim, *Phys. Rev. Lett.* **2008**, *100*, 016602.
[9] Y. B. Zhang, Y. W. Tan, H. L. Stormer, P. Kim, *Nature* **2005**, *438*, 201.
[10] P. Avouris, *Nano Lett.* **2010**, *10*, 4285.
[11] F. Schwierz, *Nature Nanotechnol.* **2010**, *5*, 487.
[12] Y. M. Lin, C. Dimitrakopoulos, K. A. Jenkins, D. B. Farmer, H. Y. Chiu, A. Grill, Ph. Avouris, *Sci.* **2010**, *327*, 662.
[13] L. Liao, J. Bai, R. Cheng, Y. C. Lin, S. Jiang, Y. Qu, Y. Huang, X. Duan, *Nano Lett.* **2010**, *10*, 3952.
[14] F. Schedin, A. K. Geim, S. V. Morozov, E. W. Hill, P. Blake, M. I. Katsnelson, K. S. Novoselov, *Nat. Mater.* **2007**, *6*, 652.
[15] M. Winter, J. O. Besenhard, M. E. Spahr, P. Novak, *Adv. Mater.* **1998**, *10*, 725.
[16] S. Kataria, A. Patsha, S. Dhara, A. K. Tyagib, H. C. Barshiliaa, *J. Raman Spectrosc.* **2012**, *43*, 1864.
[17] K. Kim, Y. Zhao, H. Jang, S. Lee, J. Kim, K. Kim, J. Ahn, P. Kim, J. Choi, B. Hong, *Nature* **2009**, *457*, 706.
[18] S. Bae, H. Kim, Y. Lee, X. Xu, J. Park, Y. Zheng, J. Balakrishnan, T. Lei, H. Kim, Y. Song, Y. Kim, K. Kim, B. Özyilmaz, J. Ahn, B. Hong, S. Lijima, *Nat. Nanotechnol.* **2010**, *5*, 574.
[19] F. Banhart, J. Kotakoski, A. V. Krasheninnikov, *ACS nano.* **2010**, *5*, 26.
[20] X. Wang, X. Li, L. Zhang, Y. Yoon, P. K. Weber, H. Wang, J. Guo, H. Dai, *Science* **2009**, *324*, 768.
[21] S. Berciaud, M. Y. Han, K. F. Mak, L. E. Brus, P. Kim, T. F. Heinz, *Phys. Rev. Lett.* **2010**, *104*, 227401.
[22] M. Freitag, M. Steiner, Y. Martin, V. Perebeinos, Z. Chen, J. C. Tsang, P. Avouris, *Nano Lett.* **2009**, *9*, 1883.
[23] C. G. Kang, S. K. Lee, Y. G. Lee, H. J. Hwang, C. Cho, S. K. Lim, J. Heo, H. J. Chung, H. Yang, S. Seo, B. H. Lee, *IEEE Electron Device Lett.* **2011**, *32*, 1591.
[24] A. C. Ferrari, J. C. Meyer, V. Scardaci, C. Casiraghi, M. Lazzeri, F. Mauri, S. Piscanec, D. Hiang, K. S. Novoselov, S. Roth, A. K. Geim, *Phys. Rev. Lett.* **2006**, *97*, 187401.
[25] L. G. Cançado, A. Jorio, E. H. Martins Ferreira, F. Stavale, C. A. Achete, R. B. Capaz, M. V. O. Moutinho, A. Lombardo, T. S. Kulmala, A. C. Ferrari, *Nano Lett.* **2011**, *11*, 3190.
[26] A. Das, S. Pisana, B. Chakraborty, S. Piscanec, S. K. Saha, U. V. Waghmare, K. S. Novoselov, H. R. Krishnamurthy, A. K. Geim, A. C. Ferrari, A. K. Sood, *Nat. Nanotechnol.* **2008**, *3*, 210 .
[27] S. Sahoo, R. Palai, R. S. Katiyar, *J. Appl. Phys.* **2011**, *110*, 044320 .
[28] S. Sahoo, G. Khurana, S. K. Barik, S. Dussan, D. Barrionuevo, R. Katiyar, *J. Phys. Chem. C* **2013**, *117*, 5485.
[29] I. Calizo, A. A. Balandin, W. Bao, F. Miao, C. N. Lau, *Nano Lett.* **2007**, *7*, 2645.
[30] D. Chae, B. Krauss, K. von Klitzing, J. H. Smet, *Nano Lett.* **2010**, *10*, 466.
[31] Z. H. Ni, H. M. Wang, Z. Q. Luo, Y. Y. Wang, T. Yu, Y. H. Wu, Z. X. Shen, *J. Raman Spectrosc.* **2010**, *41*, 479.
[32] T. M. G. Mohiuddin, A. Lombardo, R. R. Nair, A. Bonetti, G. Savini, R. Jalil, N. Bonini, D. M. Basko, C. Galiotis, N. Marzari, K. S. Novoselov, A. K. Geim, A. C. Ferrari, *Phys. Rev. B* **2009**, *79*, 205433.
[33] M. Huang, H. Yan, C. Chen, D. Song, T. F. Heinz, J. Hone, *Proc. Natl. Acad. Sci. U. S. A.* **2009**, *106*, 7304.
[34] S. Ryu, L. Liu, S. Berciaud, Y. Yu, H. Liu, P. Kim, G. W. Flynn, L. E. Brus, *Nano Lett.* **2010**, *10*, 4944.
[35] K. Kim, H. Lee, J. Choi, Y. Youn, J. Choi, H. Lee, T. Kang, M. Jung, H. Shin, H. Lee, S. Kim, B. Kim, *Adv. Mater.* **2008**, *20*, 3589.
[36] J. Baik, S. Kang, H. Hwang, C. Hwang, K. Kim, B. Kim, K. An, C. Park, H. Shine, *Surf. Sci.* **2012**, *606*, 481.
[37] G. Kresse, J. Furthmüller, *Phys. Rev. B* **1996**, *54*, 11169.

Supporting information

Additional supporting information may be found in the online version of this article at the publisher's web site.